





# Genetic Predisposition Toward Multicellularity in *Chlamydomonas reinhardtii*

I-Chen Kimberly Chen <sup>1,\*</sup>, Shania Khatri <sup>1</sup>, Matthew D. Herron <sup>1</sup>, Frank Rosenzweig <sup>1,\*</sup>

<sup>1</sup>School of Biological Sciences, Georgia Institute of Technology, Atlanta, GA, USA

\*Corresponding authors: E-mails: kichen.evol@gmail.com; frank.rosenzweig@biology.gatech.edu.

Accepted: April 28, 2025

## Abstract

The evolution from unicellular to multicellular organisms facilitates further phenotypic innovations, notably cellular differentiation. Multiple research groups have shown that, in the laboratory, simple, obligate multicellularity can evolve from a unicellular ancestor under appropriate selection. However, little is known about the extent to which deterministic factors such as ancestral genotype and environmental context influence the likelihood of this evolutionary transition. To test whether certain genotypes are predisposed to evolve multicellularity in different environments, we carried out a set of 24 evolution experiments, each founded by a population consisting of 10 different strains of the unicellular green alga *Chlamydomonas reinhardtii*, all in equal proportions. Twelve of the initially identical replicate populations were subjected to predation by the protist *Paramecium tetraurelia*, while the other 12 were subjected to settling selection by slow centrifugation. Population subsamples were transferred to fresh media on a weekly basis for a total of 40 transfers (~600 generations). Heritable multicellular structures arose in 4 of 12 predation-selected populations (6 multicellular isolates in total), but never in the settling selection populations. By comparing whole genome sequences of the founder and evolved strains, we discovered that every multicellular isolate arose from one of two founders. Cell cluster size varied not only among evolved strains derived from different ancestors but also among strains derived from the same ancestor. These findings show that both deterministic and stochastic factors influence whether initially unicellular populations can evolve simple multicellular structures.

**Key words:** multicellularity, genetic predisposition, experimental evolution, *C. reinhardtii*.

## Significance

Multicellularity has evolved in many branches across the Tree of Life, and at many times in life's history, in each case producing a new type of individual open to division of labor among its constituent cells. While these facts are beyond dispute, the ecological and genetic mechanisms that drive the transition from unicellular to multicellular life are imperfectly understood. Using the power of experimental evolution and genomics, we show that different selection pressures and different ancestral genotypes can profoundly influence whether and how a unicellular eukaryote makes the transition to primitive multicellularity.

## Introduction

A longstanding question in population biology centers around the relative roles that stochastic processes (e.g. mutation, recombination, and genetic drift) versus deterministic processes (e.g. natural selection) play in generating evolutionary trajectories and outcomes. In many instances

of convergent evolution, the deterministic process of natural selection seems to prevail (Morris 2003; Losos 2010; McGhee 2011). For example, on each of the Caribbean's four largest islands (Puerto Rico, Jamaica, Cuba, and Hispaniola), lizards of the genus *Anolis* exhibit four basic morphologies: slender grass-dwelling forms with long tails,

© The Author(s) 2025. Published by Oxford University Press on behalf of Society for Molecular Biology and Evolution.

This is an Open Access article distributed under the terms of the Creative Commons Attribution-NonCommercial License (<https://creativecommons.org/licenses/by-nc/4.0/>), which permits non-commercial re-use, distribution, and reproduction in any medium, provided the original work is properly cited. For commercial re-use, please contact [reprints@oup.com](mailto:reprints@oup.com) for reprints and translation rights for reprints. All other permissions can be obtained through our RightsLink service via the Permissions link on the article page on our site—for further information please contact [journals.permissions@oup.com](mailto:journals.permissions@oup.com).

ground-dwelling forms with long legs, short-legged forms that creep on twigs, and canopy-dwelling forms with large toe pads. These four body types independently adapted to similar habitats on each island, making it one of the best-studied examples of how evolutionary outcomes can be predictable (Losos 2010).

On the other hand, stochastic processes, such as a lineage's history, in particular its experience of mutation and drift, can make evolutionary outcomes unpredictable (Gould 1989). In *Escherichia coli* and *Salmonella typhimurium*, resistance to the antibiotic streptomycin decreases the rate of protein synthesis, which can reduce cells' fitness when the drug is absent (Schrag et al. 1997; Maisnier-Patin et al. 2002). This fitness cost can be diminished by compensatory mutations at other sites in the bacteria's genomes (Schrag and Perrot 1996; Bjorkman et al. 1999). However, many of these compensatory mutations prove detrimental when placed in wild-type, streptomycin-sensitive backgrounds, indicating that their fitness effect depends on genetic background (Schrag et al. 1997; Maisnier-Patin et al. 2002; Weinreich et al. 2005). Had those compensatory mutations occurred in lineages prior to the arrival of streptomycin-resistant mutations, their evolutionary trajectories and fitness outcomes could have been very different.

Laboratory microbial evolution has proved useful for investigating under what conditions stochastic versus deterministic factors exert the stronger influence on adaptive evolution. Well-controlled, highly replicated experiments can be carried out for hundreds or even thousands of generations under different types and/or intensities of selection. Such studies have repeatedly shown that similar environments tend to select for similar phenotypes, suggesting that evolution can be deterministic and predictable. For example, relative to their ancestor, all 12 lines in Richard Lenski's long-term evolution experiment (LTEE) in *E. coli* evolved faster growth and larger cell size (Lenski and Travisano 1994), as well as similar overall patterns of gene expression (Cooper et al. 2003). In asexual haploid *Saccharomyces cerevisiae* populations, sterility and whole genome duplication repeatedly evolved (Lang et al. 2011; Fisher et al. 2018). Of course, stochastic processes such as mutation can also produce predictable results, provided that the genetic architecture of a selectively advantageous phenotype is sufficiently complex that it can be approached via different mutational trajectories (Kvitek and Sherlock 2013).

Sometimes, stochastic events such as mutations can produce wholly unexpected outcomes. Each of the 12 *E. coli* populations in the LTEE was propagated in glucose-limiting, citrate-buffered medium. A diagnostic feature of wild-type *E. coli* is its inability to ferment citrate under oxic conditions. Remarkably, after ~31,000 generations, a weakly beneficial mutation arose in 1 of the 12 populations, which was

followed by a refining mutation that enabled cells to exploit citrate (Cit<sup>+</sup>) as a growth substrate. These mutations were strongly selected, resulting in a Cit<sup>+</sup> dominated, Cit<sup>+</sup>/Cit<sup>-</sup> population (Blount et al. 2008; Blount et al. 2012; Quandt et al. 2014). Thus, this two mutation combo, a tandem duplication that captured an aerobically expressed promoter for the expression of a previously silent citrate:succinate antiporter gene, *citT*, and a promoter mutation that activated expression of C<sub>4</sub>-dicarboxylate:H<sup>+</sup> symporter *dctA*, brought about a key evolutionary innovation (Blount et al. 2012). This innovation was contingent on an earlier mutation in the citrate synthase gene *gltA*, which in turn had benefited from even earlier mutations that increased acetate production following optimization of glucose assimilation. These observations show how a series of stochastic events can fundamentally alter a population's ecological and evolutionary trajectory (Blount et al. 2008; Quandt et al. 2015).

Laboratory microbial evolution has deepened our understanding of the roles that stochastic versus deterministic factors play in producing microevolutionary outcomes. Less clear is how these factors interact to produce macroevolutionary outcomes, such as major evolutionary transitions (Smith and Szathmary 1995). Among these is the evolution of multicellular life forms from unicellular ancestors, a transition that has occurred repeatedly across the Tree of Life (King 2004; Grosberg and Strathmann 2007; Knoll 2011; Sebe-Pedros et al. 2017), and that has served as a gateway to further innovations, such as division of labor among cells, including germ-soma differentiation (Smith and Szathmary 1995).

Historically, our understanding of what drives the evolution of multicellularity has derived from retrospective approaches such as paleontology (Gibson et al. 2018; El Albani et al. 2019; Tang et al. 2020), comparative morphology (Brunet and King 2017; Tikhonenkov et al. 2020; Umen and Herron 2021), and comparative genomics (King et al. 2008; Prochnik et al. 2010; Suga et al. 2013; Hanschen et al. 2016; Sebe-Pedros et al. 2016; Featherston et al. 2018; Paps and Holland 2018; Lindsey et al. 2024). In recent years, a number of investigators have adopted a prospective approach and shown how simple, heritable, obligate multicellularity can evolve under selection in the laboratory (Boraas et al. 1998; Becks et al. 2010; Ratcliff et al. 2012, 2013; Herron et al. 2019). Here, using laboratory evolution, we investigate how two deterministic factors, selection mode and ancestry, interact with mutation to enable a unicellular eukaryote, the green alga *Chlamydomonas reinhardtii*, to undergo the evolutionary transition from single cells to multicellularity.

*C. reinhardtii* is a member of the volvocine algae (Division Chlorophyta), a group that encompasses species exhibiting different levels of complexity that range from single-celled *C. reinhardtii*, to colonial *Gonium pectorale*, to fully

differentiated *Volvox carteri*. Two prior evolution experiments generated heritable multicellularity in *C. reinhardtii* via selective regimens that favor increased size. Using settling selection, Ratcliff et al. (2013) evolved amorphous multicellular clusters of  $>10^2$  cells bound to one another by a transparent extracellular matrix. Using predation selection by the protist *Paramecium tetraurelia*, Herron et al. (2019) evolved a variety of stereotypical multicellular structures, consisting of  $2^2$  to  $2^5$  cells surrounded by a common cell wall. These structures bear a striking resemblance to morphologies exhibited by some of the more “primitive” multicellular members of the volvocine algae, e.g. *Pandorina* and *Yamagishiella*.

Unfortunately, instead of starting from the same ancestral strains, the ancestors used in both of these selection experiments consisted of different outbred populations, making it impossible to establish whether it was the ancestral genotype or the selective regimen that determined which form of multicellularity evolved. To ascertain whether certain genotypes are predisposed to evolve certain forms of multicellularity, and/or whether different regimes favor different multicellular phenotypes, we carried out two sets of evolution experiments, each founded by the same population, which consisted of 10 different strains of *C. reinhardtii*, all in equal proportion. Twelve initially identical replicate populations were subjected to predation by *P. tetraurelia*, and 12 replicate populations were subjected to settling selection. Subsamples of these populations were transferred to fresh medium every week for a total of 40 transfers (~600 generations). Because the medium used in this experiment contains abundant nitrate and entry into the *C. reinhardtii* sexual cycle is controlled by nitrogen deprivation, we expected all reproduction to be asexual (Sager and Granick 1954). Founder strains included two lab strains and eight field isolates, each of which was phenotypically (e.g. cell sizes and chlorophyll content) and genetically different from the others (Flowers et al. 2015). Each of our founder strains contained unique stable polymorphisms that serve as markers for identifying the likely ancestor(s) of evolved multicellular strains.

After ~600 generations, heritable, obligate multicellular structures arose in 4 of 12 predation-selected populations, but never in the settling rate-selected populations. The ancestry of these multicellular strains could be traced back to only 2 of the 10 ancestors, indicating that certain genetic backgrounds may predispose the evolution of heritable multicellularity under predation. The morphology of some multicellular strains originating from the same “parent” differed markedly. Thus, stochastic processes such as mutation accumulation can lead to strikingly different multicellular forms in populations evolved under the same conditions. Together, our findings illustrate how the interplay of deterministic and stochastic factors shapes the evolutionary transition from single cells to simple multicellularity.

## Results

### Stably Heritable Multicellularity Evolved Under Predation Selection But Not Under Settling Selection

A founder population of *C. reinhardtii* was created by mixing in equal proportion each of the 10 strains described in Table 1; subsamples of this founder population were subjected to 12-fold replicated experimental evolution according to the scheme depicted in Fig. 1. Hereafter, we will refer to Predation Selection lines as PS01 to PS12 and Settling Rate Selection lines as SRS01 to SRS12. Under the predator selective regime, after 16 weekly transfers, we observed multicellular structures in 2 of the 12 replicate populations, PS05 and PS11. However, evolved isolates from those two populations did not maintain their multicellular phenotypes after serial plate transfers in the laboratory; neither did multicellular morphologies persist in these two populations in the following screen after 8 weeks.

After 32 weekly transfers, multicellular structures appeared in three populations, PS09, PS10, and PS11; one evolved strain was isolated from each population (PS09-32-A, PS10-32-B, and PS11-32-B, respectively). Other than PS10-32-B from PS10, the multicellular strains that evolved in populations PS09 and PS11 after 32 weekly transfers maintained multicellular morphologies after being plated on solid medium three times in succession, as well as in the experiments described below (Fig. 2a and b). After an additional 8 weekly transfers (40 transfers altogether), multicellular structures were detected in two other predation-selected populations, PS02 and PS12; three evolved strains were isolated from PS02 (PS02-40-A, PS02-40-B, and PS02-40-C), and one strain was isolated from PS12 (PS12-40-C). Each of the evolved strains isolated from PS02 and PS12 after 40 weekly transfers maintained their multicellular structures after being plated on solid

**Table 1** *C. reinhardtii* founder strains used in this experiment

Strain	Mating type <sup>a</sup>	Origin	Location	Reference(s)
CC-1690	mt+	Lab	—	Sager (1955)
CC-5080	mt–	Lab	—	Gallaher et al. (2015)
CC-2937	mt+	Field	Quebec, Canada	Sack et al. (1994)
CC-2936	mt+	Field	Quebec, Canada	Sack et al. (1994)
CC-2935	mt–	Field	Quebec, Canada	Sack et al. (1994)
CC-2344	mt+	Field	Ralston, PA	Spanier et al. (1992)
CC-2342	mt–	Field	Pittsburgh, PA	Spanier et al. (1992)
CC-2343	mt+	Field	Melbourne, FL	Spanier et al. (1992)
CC-2931	mt–	Field	Durham, NC	Proschold et al. (2005)
CC-2290	mt–	Field	Minnesota	Gross et al. (1988)

<sup>a</sup>There are two mating types, identical in appearance and known as mating type *plus* and *minus*, in *C. reinhardtii*. The + or – sign in each parenthesis denotes the mating type of each strain. The entry into the sexual cycle is controlled by nitrogen deprivation in *C. reinhardtii*. The media used in the experiment sustain normal cell growth and we expect all reproduction to be asexual.

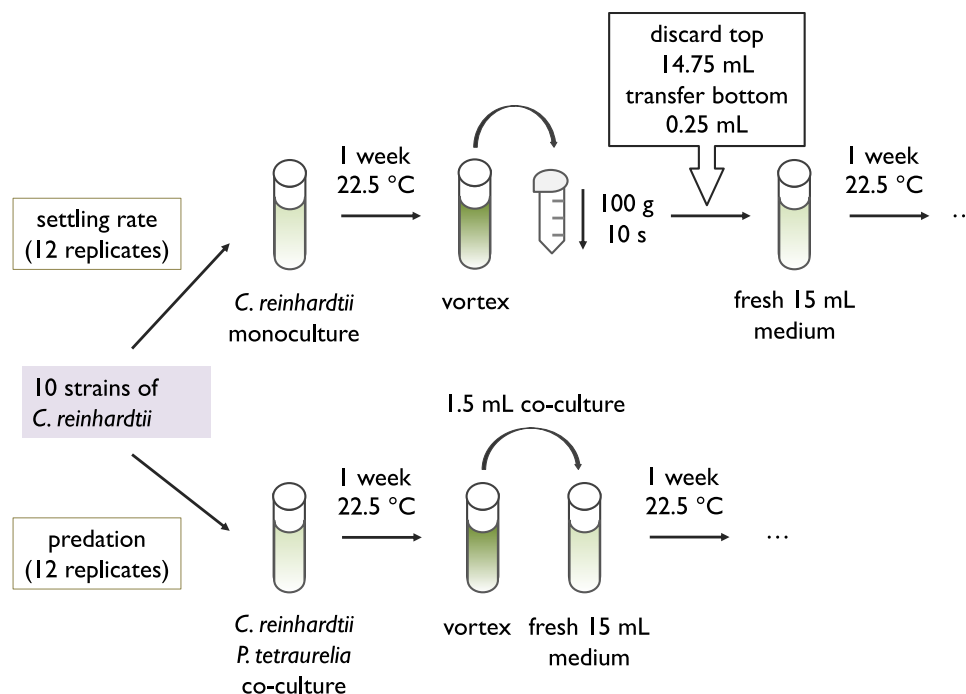


**Fig. 1.** Experimental evolution diagram. A founder population consisting of 10 different strains of *C. reinhardtii*, all in equal proportion, was used to generate 24 replicate populations: 12 were subjected to settling selection that favors large cell clusters that settle rapidly; 12 were subjected to predation by the protist *P. tetraurelia*. Subsamples of each population were transferred to fresh medium every week, with approximately 15 generations elapsing between transfers, for a total of 40 transfers. For the settling rate selection, each population was transferred to a 15 mL Falcon tube and centrifuged at  $100\times g$  for 10 s and only the bottom 0.25 mL was transferred to fresh medium. For populations under predation selection, 1.5 mL of co-cultured *C. reinhardtii* and *P. tetraurelia* were transferred to fresh medium every week.

medium three times in succession, as well as in the experiments described below (Fig. 2c to f). In summary, stably heritable multicellular phenotypes were observed in 4 of 12 populations evolved under predation selection.

Under the settling rate selection regimen, we observed multicellular structures in 2 of the 12 replicate populations, SRS05 and SRS07, after 16 weekly transfers, and again in populations SRS03, SRS08, and SRS11 after 32 weekly transfers. However, none of these isolates maintained multicellular phenotypes after serial plate transfers in the laboratory. Thus, stably heritable multicellular phenotypes were never observed in any of the settling rate-selected populations over the course of 40 weekly transfers, or ~600 generations.

### Multicellular Phenotypes Arise as Clones

In the unicellular ancestors, most cells exist as single cells in their respective populations (Fig. 2g and h). By contrast, within each multicellular structure of the evolved strains, cell walls are visible surrounding individual two, four, or eight cells, and these are held in place by a transparent extracellular matrix (Fig. 2a to f). Most evolved strains form clusters approximately 20 to 100  $\mu\text{m}$  in size, except PS09-32-A, which can form clusters whose diameters range up to several hundred micrometers (Fig. 2a). Development

in the evolved multicellular strains is strictly clonal. Time-lapse microscopy over 72 h shows that, compared with the ancestors where dividing cells only transiently form clusters before daughter cells are released (e.g. CC-2936, [supplementary video S1, Supplementary Material online](#)), multicellular isolates develop by parental cells dividing into daughter cells within clusters over multiple rounds of cell division ([supplementary videos S2 to S7, Supplementary Material online](#)). Because cells within each multicellular cluster are genetically identical, clusters likely function as units of selection (Lewontin 1970; Michod and Roze 2001) under predation selection.

### Multicellular Isolates Exhibit Strain-Specific Differences in Size and Cell Number

In order to determine cluster size distributions for evolved strains, we sampled, stained, and imaged growing cultures every 24 h over a 6-d period, which approximated the serial transfer interval of our evolution experiments. Four biological replicates were performed for each of the evolved strains, and two biological replicates were performed for the ancestral strains. As distributions tended to be right-skewed, data were represented as boxplots that depict clusters' central tendencies. Large outlier clusters were occasionally present in each population. These outliers,

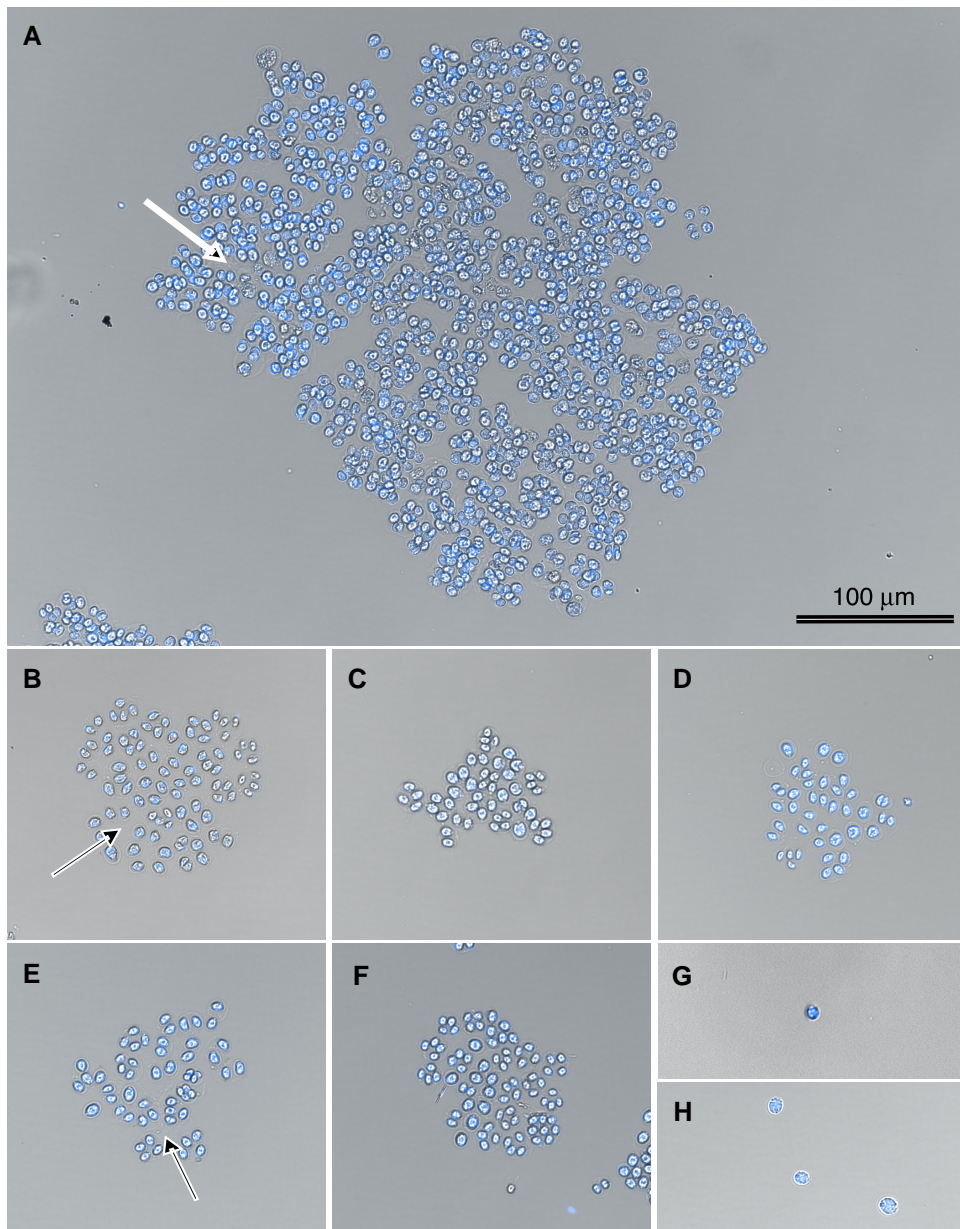


**Fig. 2.** Microscopic images of each evolved strain and their unicellular ancestors stained by DAPI. a) PS09-32-A; b) PS11-32-B; c) PS02-40-A; d) PS02-40-B; e) PS02-40-C; f) PS12-40-C; g) CC-2936; and h) CC-1690. Black arrows indicate examples of extracellular matrix. Genomic data indicate that strain PS12-40-C evolved from CC-1690, while the rest of multicellular strains evolved from CC-2936 (see Table 3).

defined as data points that exceeded a distance of 1.5 times the interquartile range (IQR) above the third quartile, were excluded from further analyses.

We observed that multicellular cluster size varied among evolved strains over the course of 6 d. The median cluster size of multicellular strain PS09-32-A was  $>80$  cells on day 1 and then maintained at  $>100$  cells throughout the growth cycle, with a maximum of 156 cells on day 6 (Fig. 3a). By contrast, median cluster sizes of PS11-32-B, PS02-40-A, PS02-40-B, and PS12-40-C ranged between two and ten cells, with maximum sizes being reached on

day 1 (6, 10, 7, and 7 cells, respectively) then gradually decreasing thereafter (Fig. 3b, c, d, and f). The median cluster size of strain PS02-40-C remained at four cells between day 1 and day 5 before declining to two cells on day 6 (Fig. 3e). Median cluster sizes of the ancestral strains (CC-2936 and CC-1690, see the following paragraph for identification details) remained one cell per cluster over growth cycle, with multicellular clusters occurring occasionally during reproduction (Fig. 3g and h). The cluster size data used to generate Fig. 3 are provided in [supplementary Data S1, Supplementary Material](#) online.

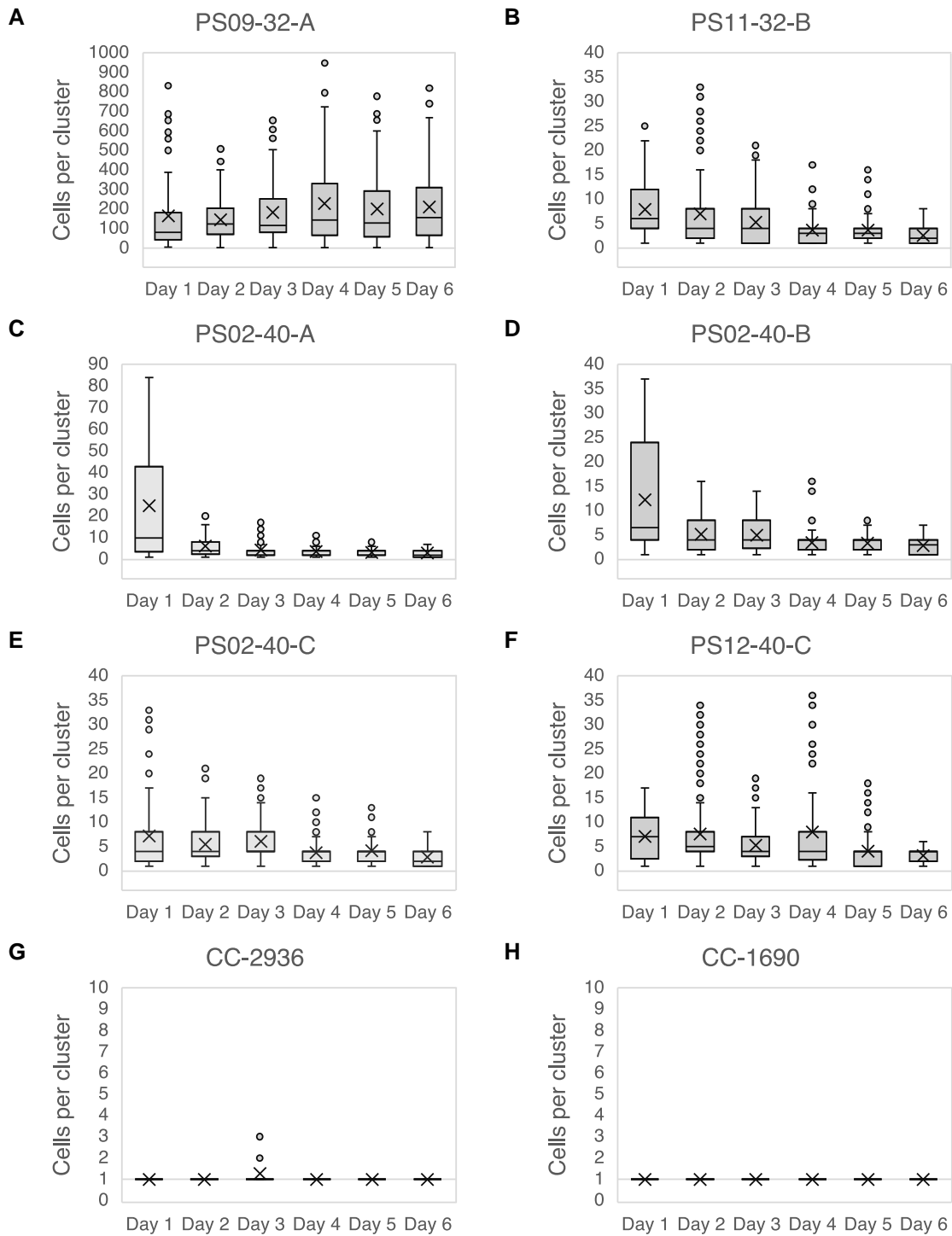


**Fig. 3.** Box plots of cells per cluster over a 6-d period. Cluster sizes were measured by sampling cultures over 6 d of growth, staining nuclei with DAPI, and imaging using fluorescent microscopy. a to f) Cluster sizes in the evolved strains and g and h) cluster sizes in the ancestors. An x or cross represents the mean of cells per cluster; the crossbar indicates the median of cells per cluster. The gray horizontal bar in each figure represents one cell per cluster. Note that the y-axis scales vary among strains.

We found that there was a significant difference among evolved strains and ancestral strains in the median cluster sizes (Kruskal–Wallis test,  $H = 242.22$ ,  $df = 7$ ,  $P << 0.01$ ).

To ensure our comparisons were of similar developmental stages, the median for each strain was measured at the time point at which it reached its maximum value, as in

**Table 2** *P*-values for Dunn's test for all pairwise comparisons between the maximum cluster sizes in different strains

	Maximum cluster size (median)							
	PS09-32-A (156 cells)	PS11-32-B (6 cells)	PS02-40-A (10 cells)	PS02-40-B (7 cells)	PS02-40-C (4 cells)	PS12-40-C (7 cells)	CC-2936 (1 cell)	CC-1690 (1 cell)
PS09-32-A	...	**	*	**	**	**	**	**
PS11-32-B	...	...	0.56	0.81	0.40	0.48	**	**
PS02-40-A	...	...	...	0.72	0.28	0.31	**	**
PS02-40-B	...	...	...	...	0.38	0.43	**	**
PS02-40-C	...	...	...	...	...	0.98	**	**
PS12-40-C	...	...	...	...	...	...	**	**
CC-2936	...	...	...	...	...	...	...	0.24
CC-1690	...	...	...	...	...	...	...	...

Single asterisks indicate *P*-values of <0.05. Double asterisks indicate *P*-values of <0.01.

Herron et al. (2019). Particularly, the median cluster size of PS09-32-A (156 cells) was significantly larger than those of other multicellular strains (6, 10, 7, 4, and 7 cells from PS11-32-B, PS02-40-A, PS02-40-B, PS02-40-C, and PS12-40-C, respectively) and those of their ancestors (1 and 1 cell from CC-2936 and CC-1690) (Table 2). There were no significant differences in median cluster sizes among all the multicellular strains other than PS09-32-A (Table 2).

#### Multicellular Isolates Evolved From Only Two of the Ten Founder Strains: CC-2936 and CC-1690

PCR analysis of mating types in the evolved multicellular isolates revealed that all were mt+, suggesting that they originated from at least one of the mt+ founder strains (supplementary fig. S1, Supplementary Material online). Therefore, for the following genomic analysis, we only compared evolved isolates with mt+ founders to identify which ancestor genotype(s) they were most likely to have originated from. We performed whole genome sequencing of PS09-32-A, PS11-32-B, PS02-40-A in PS02, and PS12-40-C to an aligned sequencing depth of ~15x, 15x, 14x, and 18x using paired end (2 × 151 bp) Illumina sequencing. One of the mt+ founder strains, CC-1690, was re-sequenced for a separate study (not published) to an aligned depth of 44x using the same Illumina sequencing method. We did not sequence PS2-40-B and PS2-40-C in PS02 owing to the fact that they are phenotypically similar to PS02-40-A, and are likely the same genotype as PS2-40-A, or only differ by a few mutations, as they were isolated from the same population. For the remaining four mt+ founder strains, their sequenced reads were downloaded from NCBI using accession numbers SAMN03272879, SAMN03272875, SAMN03272877, and SAMN03272872 for strains CC-2937, CC-2936, CC-2344, and CC2343, respectively (Flowers et al. 2015). Based on the sequence alignments to ~112 Mb of the *C. reinhardtii* CC-503 mt+ reference genome (Merchant et al. 2007), we generated a filtered genetic variant dataset that consisted of 4,714,560

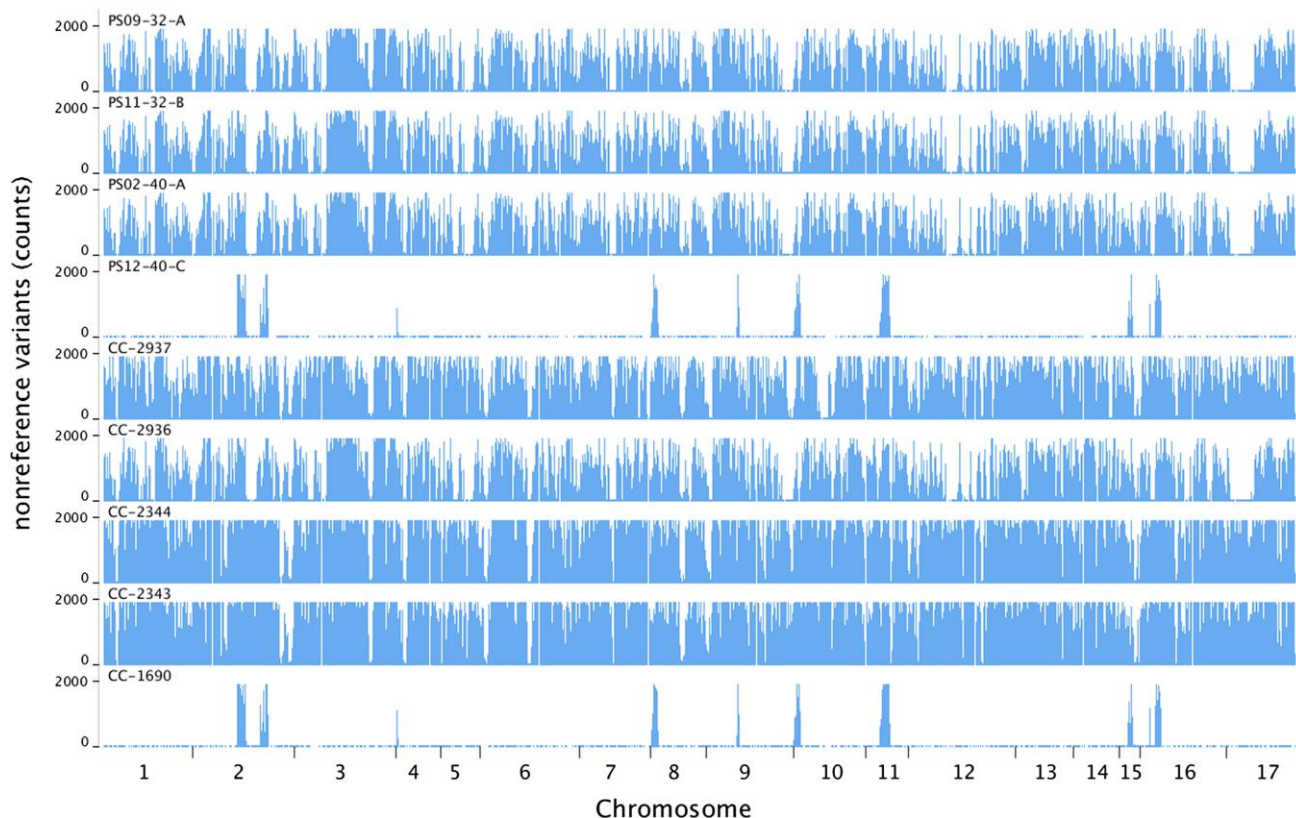
nonreference variants in all strains together. Each strain contains a genome fingerprint based on the location of their genetic variants across 17 *C. reinhardtii* chromosomes. By visually comparing the genome-wide distributions of those variants and through direct comparisons, we can infer the most likely ancestors of evolved multicellular isolates in the populations PS02, PS09, PS11, and PS12.

Among mt+ founder strains, lab strain CC-1690 is diverged from reference strain CC-503 by 90,242 variants in our filtered dataset, while the field isolates CC-2937, CC-2936, CC-2344, and CC-2343 differ from CC-503, respectively, by 1,651,964, 1,194,250, 2,102,758, and 2,187,600 variants in 111,098,438 sites across the reference genome (Table 3). Among evolved strains, PS09-32-A, PS11-32-B, and PS02-40-A contain 1,169,953, 1,110,266, and 1,144,326 nonreference variants, respectively, while PS12-40-C only contains 77,708 variants (Table 3). When comparing the genome-wide distributions of nonreference variants between mt+ founders and evolved strains, we found that the distributions in PS09-32-A, PS11-32-B, and PS02-40-A visually match to that in CC-2936, while the distribution in PS12-40-C visually match to that in CC-1690 (Fig. 4). When directly comparing the variants between mt+ founders and evolved strains, we found that >99% of variants identified in the evolved strains PS09-32-A, PS11-32-B, and PS02-40-A matched to the founder strain CC-2936, while 100% of the variants identified in PS12-40-C matched to the founder strain CC-1690 (Table 3), suggesting that PS09-32-A, PS11-32-B, PS02-40-A evolved from CC-2936, and PS12-40-C evolved from CC-1690. The <1% of variants in PS09-32-A, PS11-32-B, and PS02-40-A that did not match to CC-2936 is likely due either to different sequencing methods (e.g. CC-2936 was previously sequenced at 2 × 51 bp length using the Illumina HiSeq 2000 sequencer (Flowers et al. 2015), while the evolved strains here were sequenced at 2 × 151 bp length using the Illumina NextSeq 2000 sequencer), or to mutations that accumulated in these lines since they were sequenced by Flowers et al. (2015).

**Table 3** Comparisons between genomic variants in evolved and mt+ founder strains

	CC-1690 (90,242)	CC-2937 (1,651,964)	CC-2936 (1,194,250)	CC-2344 (2,102,758)	CC-2343 (2,187,600)
PS09-32-A (1,169,953)	59.56%	35.46%	99.93%	22.50%	18.41%
PS11-32-B (1,110,266)	59.15%	35.11%	99.90%	22.28%	18.18%
PS02-40-A (1,144,326)	59.59%	35.40%	99.93%	22.42%	18.32%
PS12-40-C (77,708)	100%	2.02%	3.58%	1.33%	1.09%

The numbers in parenthesis after strain names indicate the number of nonreference variants identified in each strain (see Methods). Heat maps are color-coded (light gray/low percentage match < gray/middle percentage match < dark gray/high percentage match).

**Fig. 4.** Genome-wide distributions of nonreference variants on 17 *Chlamydomonas* chromosomes in evolved and mt+ founder strains.

To further illustrate that specific allele combinations in the founder strains CC-2936 and CC-1690 are also present in their respective evolved isolates, Table 4 lists 25 loci across different chromosomal locations that differ among five mt+ founders. The nucleotides in those 25 positions in PS09-32-A, PS11-32-B, and PS02-40-A all match to the ones in CC-2936, while the nucleotides in those positions in PS12-40-C all match to CC-1690 (Table 4), indicating that CC-2936 is the ancestor of PS09-32-A, PS11-32-B, and PS02-40-A and that CC-1690 is the ancestor of PS12-40-C. Further, because the founder CC-1690 was re-sequenced about the time we started the evolution experiments, we were able to identify the mutations accumulated in its evolved strain PS12-40-C. There are 12 candidate mutations (read depth  $\geq 5\times$ , allele frequencies  $> 0.85$ ); one of them is a missense mutation (arginine to leucine) in a gene

encoded for a putative protein (Cre13.g592551), while the rest of the mutations are in introns or intergenic regions (supplementary table S1, Supplementary Material online). The results here hence serve as a foundation for future genetic studies to elucidate the genetic basis for the multicellular phenotype in PS12-40-C.

## Discussion

The emergence of multicellular organisms and the emergence of eukaryotes are widely regarded as major evolutionary transitions in the history of life (Smith and Szathmary 1995; Herron 2021). However, unlike eukaryogenesis, which seems to have been a singular event (Andersson et al. 1998; Wang and Wu 2015), multicellularity has arisen at least 25 times across widely divergent



**Table 4** Examples of genomic variants that differ among mt+ founder strains and their presence and absence in the evolved strains

Strain position	CC-1690	CC-2937	CC-2936	CC-2344	CC-2343	PS09-32-A	PS11-32-B	PS02-40-A	PS12-40-C
Chrom_1 1782815	A	T	T	T	T	T	T	T	A
Chrom_1 1796517	A	G	A	A	A	A	A	A	A
Chrom_2 531304	G	G	A	G	G	A	A	A	G
Chrom_2 906332	T	T	T	C	T	T	T	T	T
Chrom_2 1216720	C	C	C	C	T	C	C	C	C
Chrom_3 666196	C	A	T	A	A	T	T	T	C
Chrom_3 983155	AA	AG	GG	GG	AG	GG	GG	GG	AA
Chrom_3 1128242	C	C	T	C	C	T	T	T	C
Chrom_4 14191	TGA	TGA	TGA	TA	TGA	TGA	TGA	TGA	TGA
Chrom_4 236504	G	G	G	G	A	G	G	G	G
Chrom_5 763807	G	A	A	A	A	A	A	A	G
Chrom_5 888052	C	T	C	C	C	C	C	C	C
Chrom_5 1624406	G	G	A	G	G	A	A	A	G
Chrom_6 122423	ACG	ACA	ACA	ATG	ACG	ACA	ACA	ACA	ACG
Chrom_6 204099	T	T	T	T	C	T	T	T	T
Chrom_7 1392564	CCCGC	CC	CC	CC	CC	CC	CC	CC	CCCGC
Chrom_8 301955	TG	AA	TG	TG	TG	TG	TG	TG	TG
Chrom_8 533535	A	A	G	A	A	G	G	G	A
Chrom_9 133015	A	A	A	C	A	A	A	A	A
Chrom_10 69703	C	C	C	C	T	C	C	C	C
Chrom_11 448221	A	C	C	C	C	C	C	C	A
Chrom_13 679947	ATCTAT	AAC	ATCTAT	AAC	AAC	ATCTAT	ATCTAT	ATCTAT	ATCTAT
Chrom_14 153285	G	G	A	G	G	A	A	A	G
Chrom_15 135507	C	C	C	T	C	C	C	C	C
Chrom_16 312391	C	C	C	C	G	C	C	C	C

lineages (Grosberg and Strathmann 2007). Within the volvocine algae, multicellularity arose in some lineages as recently as the Jurassic and Cretaceous periods (126 to 49 million years ago) (Herron et al. 2009; Lindsey et al. 2021; Ma et al. 2023; Lindsey et al. 2024). Still, even though multicellularity has arisen repeatedly and in diverse lineages, little is known about the relative roles that stochastic versus deterministic factors play in driving this transition. Previous work has shown that in the lab simple, obligate multicellularity can evolve in the unicellular green alga *C. reinhardtii* under either settling or predation selection (Ratcliff et al. 2013; Herron et al. 2019).

Here, we used experimental evolution to assess the influences that ancestry and selective environment have on whether single cells become stably multicellular. We established a founder population consisting of 10 different strains of *C. reinhardtii*, all in equal proportion. This founder population was used to generate 24 replicate populations: 12 were subjected to predation by the protist *P. tetraurelia*, 12 were subjected to settling selection that favors large cell clusters that settle rapidly. After ~600 generations, heritable, obligate multicellular structures arose in 4 of 12 predation-selected populations, but never in the settling rate-selected populations. Further, we found that multicellular isolates evolved from only two founders CC-1690 and CC-2936, and that the size and structure of one of the multicellular isolates from the founder CC-2936 differed

from others. Whether the obligate multicellularity we observed was at a stable point or at some point along a continuum of evolving multicellularity, our results indicate that not only deterministic but also stochastic factors play significant roles in the trajectories by which populations evolve multicellularity.

If the evolutionary transition to multicellularity was purely deterministic, we would expect that similar selective environments would result in similar phenotypes regardless of ancestry. Indeed, we observed similar types of multicellularity evolved under predation selection in PS02-40-A, PS11-32-B, and PS12-40-C, even from different ancestors, indicating that deterministic factors are a dominant force in our evolution experiments. However, the fact that we observed a different type of multicellularity evolved under predation selection, even from the same ancestor (CC-2936, started as a single, isolated colony for the evolution experiments here), suggests that stochastic processes such as the accumulation of random mutations can lead to largely different outcomes. That being said, the large clusters formed by PS09-32-A (>100 cells most of the time) can be costly: colony growth may be limited because interior cells do not have the same access to nutrients or environmental signals (e.g. oxygen or light) compared with exterior cells (Bonner 2011; Knoll and Hewitt 2011). If this is true, then it is possible that PS09-32-A might have evolved a smaller cluster size similar to what we observed in other

multicellular isolates had we allowed the experiment to run longer. Such a response to selection would demonstrate that the evolutionary process is still deterministic at the phenotypic level.

We also found that the multicellular isolates evolved in 3 of 12 predation-selected populations originated from founder CC-2936, while the multicellular isolates evolved in the other predation-selected population descended from founder CC-1690. We did not observe multicellular isolates evolved from any other founders. This outcome suggests that particular suites of genetic variants had accumulated in those strains prior to our evolution experiments, and that these facilitated the transition to multicellularity in our selective regimen. An inverse question to ask is: why are some founders more resistant than others to selection pressures expected to favor the evolution of multicellularity? Were the populations quickly purged of certain founders just because they grew less quickly or to a lower stationary phase density? In other words, were the results biased at the onset because some strains have poor competitive ability, relative to others? To test for these possibilities, future work should be directed toward competition experiments among founders, and/or similar evolutions using the same founders, but with populations being sequenced at different time points to monitor changes in the frequency of allelic markers by which founders can be readily differentiated.

Multiple reasons could explain why multicellularity did not evolve under our settling selection regimen. First, in our experiments, settling rate selection was episodic, occurring only once a week, whereas predation selection was continuous. Second, our settling rate selection (centrifugation at 100 *g* for 10 s, with pelleted cells transferred to fresh medium once a week) differed slightly from that of Ratcliff et al. (2013) (100 *g* for 5 s, with pelleted cells transferred every 3 d). Third, so that the two treatments could be compared it was essential that the settling selection and the predation experiments be carried out in the same medium. We elected to use COMBO, a defined freshwater medium for co-culturing algae and zooplankton (Kilham et al. 1998) that had been used successfully in our earlier predation experiment (Herron et al. 2019). Significantly, COMBO does not contain an organic carbon source; therefore, it only supports photoautotrophic growth of *C. reinhardtii* (Harris 2009). In this key respect, COMBO differs from the TAP medium more commonly used in *Chlamydomonas* research (including the Ratcliff et al. (2013) settling selection experiment). TAP contains acetate, which supports heterotrophic growth by *C. reinhardtii*. COMBO necessarily brings about a different physiological state than TAP, and this difference may influence *C. reinhardtii*'s latent tendency to form clonal assemblages and/or extracellular matrices that cause bodies to settle rapidly in aqueous media. Fourth, by luck of the draw, we might not have initiated our

experiment with the right set of ancestral genotypes, or with sufficient standing genetic variation. Ratcliff et al. (2013) initiated their evolutions using an outbred population that had a high level of standing genetic variation; moreover, all populations went through one round of sexual reproduction (within-population mating) during the evolutions. After 73 transfers (~315 generations) with settling rate selection imposed every 3 d, multicellular *C. reinhardtii* evolved in only 1 of 10 replicate populations. The difference between our results and those of Ratcliff et al. (2013) suggests that the amount of standing genetic variation might play a role in the tempo and mode by which multicellularity emerges. Finally, perhaps multicellularity did not evolve under the settling selection here simply because the outcome is stochastic. After all, in Ratcliff et al. (2013), only one of ten replicate populations evolved multicellularity under settling selection. If we use this as an estimate of the probability of multicellularity evolving under settling selection, the binomial probability of 0 of 12 replicates evolving multicellularity would be 0.28 ( $P(x = 0)$  given 12 trials, each with a probability of success of 0.1), far too likely to rule out.

Regarding the genetic basis of multicellularity in our experiments, we only sequenced evolved isolates exhibiting multicellularity at low coverages (14 to 18x), as our objective was to determine ancestry. Evolved unicellular isolates, in particular ones sharing a common ancestor with the evolved multicellular isolates, were not sequenced due to budget constraints. For the same reason, most of the founder strains used to start the evolution experiments were not re-sequenced; instead, we used the sequencing reads deposited at NCBI by Flowers et al. (2015). Therefore, systematic comparisons between unicellular and multicellular evolved isolates, or between founder strains and their evolved multicellular isolates, are not possible here for investigating the mutational trajectories to multicellularity. That being said, we did periodically archive subsamples of our experimental populations at -20 °C. Whole genome sequencing of those intermediate populations in the future will help illuminate how stochastic processes such as random mutations led to different outcomes in the development of obligate multicellularity, as well as when CC-1690 and CC-2936 became predominant in the evolved populations. Another approach to identify mutation(s) responsible for multicellularity would be to repeatedly backcross the multicellular trait(s) into the founder or wild-type strains to generate near isogenic lines, and then compare the genomes of the resulting lines to the founder or wild-type strains. For multicellular strains PS09-32-A, PS11-32-B, and PS02-40-A, it would also be possible to directly sequence candidate genes in which mutations are known to produce multicellular phenotypes. For example, previous work has shown that the retinoblastoma (*RB*) cell cycle regulatory pathway is involved in cluster

formation in the alga *Gonium*, an undifferentiated colonial relative of *Chlamydomonas* (Hanschen et al. 2016). Indeed, expression of the *Gonium RB* gene in a *Chlamydomonas* strain lacking its *RB* gene caused this mutant to form colonial assemblies containing 2 to 16 cells (Hanschen et al. 2016). It is possible that mutations in cell cycle genes such as *RB* may underlie the transition from unicellular to multicellular phenotypes in some of our evolution experiments.

Taken together, our findings show that genetic changes that have accumulated in certain strains of *Chlamydomonas* can shift the probabilities of alternative evolutionary paths toward multicellularity. Our results further demonstrate that de novo mutations arising under selection also play a role in shaping divergent multicellular forms, even among replicate populations evolved under the same conditions.

## Materials and Methods

### Experimental Evolution

A list of the *C. reinhardtii* founder strains used in this study is provided in Table 1. Strains were selected on the basis of their geographic isolation from one another, their phenotypic and phylogenetic diversity, and the fact that the genome of each strain has been sequenced (Flowers et al. 2015). The selected strains were ordered from the Chlamydomonas Resource Center (<https://www.chlamycollection.org/>). In this study, each founder strain received from the Chlamydomonas Resource Center was first streaked on TAP 1.5% agar plates (Gorman and Levine 1965), and a single colony was isolated and grown to stationary phase ( $\sim 6$  to  $8 \times 10^6$  cells/mL) in TAP liquid medium. Equal volumes of each founder cultures were mixed and used as the master stock to start the selection experiment. Twelve replicate populations were subjected to predation selection by *Paramecium tetraurelia* (Carolina Biological Catalogue #131560), as described by Herron et al. (2019), and 12 replicate populations were subjected to settling rate selection (Ratcliff et al. 2013) (Fig. 1). Each population was cultured on a 14:10-h light:dark cycle at 22.5 °C in 15 mL of COMBO medium. COMBO is a freshwater medium suitable for co-culturing algae and zooplankton (Kilham et al. 1998). We used COMBO for both predation and settling rate selection experiments so that the two treatments could be compared. Subsamples of each population were transferred to fresh COMBO medium every week for a total of 40 transfers, with approximately 15 generations elapsing between transfers. For experiments under predation selection, 1.5 mL of co-cultured *C. reinhardtii* and *P. tetraurelia* were transferred to fresh medium every week. For the settling rate selection, each population was transferred to a 15 mL Falcon tube and centrifuged at

100 × g for 10 s, and only the bottom 0.25 mL was transferred to fresh medium. Under both types of selection, the bottleneck size at each transfer was approximately 1 to  $2 \times 10^6$  cells.

Every 2 months (i.e. every 8 transfers or 120 generations), 0.1 mL samples of each experimental population were diluted 100-fold, and 30 μL was plated on TAP 0.5% agar to screen for multicellular isolates. Unicellular isolates are normally motile and form large colonies on 0.5% agar plates, whereas multicellular isolates are normally non-motile and form small colonies (preliminary data not shown). Three small colonies per population (presumably multicellular isolates labeled “A”, “B”, and “C”) were picked up using sterile toothpicks, inoculated into 2 mL of TAP medium in 24-well plates, incubated overnight and screened the next day for multicellular phenotypes by visual examination under light microscopy. Isolates that demonstrated multicellular phenotypes were diluted 10-fold, then 30 μL was replated on solid medium. The same procedure was repeated three times sequentially to ensure that each isolate was clonal and that multicellular phenotypes of isolates from the predation treatment were not transiently induced by the presence of the *P. tetraurelia* predator. All founder strains used to start the evolution experiment and evolved multicellular isolates were cryopreserved at –80 °C using the GeneArt Cryopreservation Kit for Algae (Invitrogen, Thermal Fisher Scientific). In addition, every 2 months, we archived subsamples of our experimental populations at –20 °C for future whole genome bulk sequencing to track the changes in frequency of different founder strains. We chose freezing subsamples at –20 °C rather than cryopreserving at –80 °C because it has been shown that different genotypes of *C. reinhardtii* exhibit different degrees of resilience to cryopreservation, and strains cannot be revived from polyclonal populations in the proportions originally cryopreserved (Boswell et al. 2021). Faced with this limitation, we did not attempt to cryopreserve intervening populations, which were undoubtedly polyclonal.

### Cells per Cluster in the Multicellular Isolates

At the end of our evolution experiments, we obtained pure culture isolates of several multicellular strains. To understand how cluster size distribution patterns varied among strains over a 6-d incubation period as well as the maximum number of cells per cluster, we subjected each strain to epifluorescence microscopy. Cells of evolved strains and their ancestors were scraped from TAP 1.5% agar plates (3 to 4 inoculation loops, 0.09 cm in diameter), inoculated into 15 mL of TAP medium then cultured for 5 d to high density (approximately 6 to  $8 \times 10^6$  cells/mL). Next, we transferred cultures of each strain into 15 mL of TAP medium at a starting density of  $10^4$  cells/mL, cultured on a 14:10-h light:dark

cycle at 22.5 °C, and sampled every 24 h over the course of 6 d. We used TAP medium here because it is a standard medium commonly used in *Chlamydomonas* research (Gorman and Levine 1965); multicellular phenotypes were stable in TAP. Subsets of cell cultures were removed from well-mixed test tubes and transferred into 1.5 mL Eppendorf tubes (from day 1 to day 6, the amounts of cell cultures transferred were 1,200, 900, 400, 300, 200, and 100  $\mu$ L). Samples were centrifuged at 14,000  $\times$  *g* for 1 min and the supernatant was replaced by a 50% v/v ethanol-water solution to fix cells and render cell membranes permeable to the fluorescent nucleotide stain DAPI (4',6-diamidino-2-phenylindole). After a 10-min fixation period, samples were centrifuged again at 14000  $\times$  *g* for 1 min and the supernatant was replaced with distilled water containing 1  $\mu$ g/mL DAPI. Cells stained with DAPI were kept in the dark for 1 h at 25 °C, then moved to a 4°C refrigerator without light to prevent photobleaching until being imaged on an inverted epifluorescence microscope (the Eclipse Ti series, Nikon).

Prior to imaging, samples were removed from the refrigerator and gently pipetted. A 10  $\mu$ L aliquot of each sample was mounted on glass microscope slides, then multiple images were recorded at 20 $\times$  magnification using bright-field and the DAPI filter set (Excitation/Emission: 358/461 nm) overlapping on top of each other. Images were taken of at least 20 clusters or cells per sample, providing a robust dataset for computing the distribution of cluster sizes within each population at a given time point. Next, images were manually screened to demarcate cluster boundaries and record cell numbers within each boundary using Cell Counter in ImageJ (<https://imagej.nih.gov/ij/>). Cell number was estimated by counting DAPI-stained nuclei confined within cluster boundaries (e.g. Fig. 2). This procedure was repeated four times for each of the evolved strains and twice for the ancestral strains.

### Modes of Reproduction in Multicellular Isolates

Multicellularity can arise either by many cells aggregating (Bonner 2000; Du et al. 2015) or by one cell reproducing clonally and its daughter cells remaining intimately associated (Bonner 1998; Tarnita et al. 2013). In order to distinguish between these two forms of multicellularity, ancestral and evolved strains were imaged using time-lapse transmission microscopy over 72 h of growth. As before, cells were scraped from TAP 1.5% agar plates (3 to 4 inoculation loops, 0.09 cm in diameter), inoculated into liquid TAP medium and cultured for 5 d to high density (approximately 6 to 8  $\times$  10<sup>6</sup> cells/mL). Then, each culture was vortexed, transferred 1:100 into fresh TAP medium, and allowed to grow for two more days. Exponentially growing cultures were first mixed by vortexing, then diluted 1:10 in TAP medium, whereafter 100  $\mu$ L from each culture was inoculated into

the wells of a 96-well tissue culture plate containing 100  $\mu$ L of TAP medium per well. Well positions for each strain were determined by a random number generator. Wells not inoculated with algae were filled instead with 100  $\mu$ L of TAP cell-free medium. For time-lapse microscopy, the 96-well plate was imaged at 200 $\times$  magnification using the Nikon Eclipse Ti inverted microscope, where the field of view was positioned on cells near the center and at the bottom of wells. The time-lapse was run for 72 h, capturing images of each well every 30 min. For each strain, five technical replicates were performed on the 96-well plate.

### Identifying the Ancestors of Evolved Multicellular Isolates

#### Mating Type Assay

To ascertain whether certain ancestral strains were more likely to evolve multicellularity than others, we identified alleles that differed among founder strains (such that each strain has a specific combination), and used those alleles as markers to determine the probable ancestor(s) of evolved multicellular strains. We first established the alleles at the mating type locus in evolved isolates, as the mating types of the founder strains had been previously identified. Each evolved isolate was subjected to PCR-amplification using either the *mid* or *fus1* locus (the *mid* gene is unique to mating type minus (mt<sup>-</sup>) cells, while the *fus1* is unique to mating type plus (mt<sup>+</sup>) cells). The *mid* locus was amplified using the primer pair MTM1F (CTG CTG GTA CAA AGG TGT GGC ACG) and MTM2R (CAT GCA GTC TCT CTC ACC CAT TCG GC), which were expected to produce a 750 bp piece of the *mid* gene; the *fus1* locus was amplified using the primer pair MTP2F (GCT GGC ATT CCT GTA TCC TTG ACG C) and MTP2R (GCG GCG TAA CAT AAA GGA GGG TCG), which were expected to produce a 434 bp piece of the *fus1* gene (Zamora et al. 2004). After identifying the mating type of evolved isolates, we next compared how their whole genome sequences differed from the founder strains, giving us deeper insight into which ancestors produced multicellular isolates.

#### Whole Genome Sequencing

Genomic DNA from evolved isolates and the ancestral strain CC-1690 (a wild-type strain in our lab) was extracted, using the *Chlamydomonas* DNA extraction protocol recommended by the Joint Genome Institute (<https://www.pacb.com/wp-content/uploads/2015/09/Experimental-Protocol-DNA-extraction-of-Chlamydomonas-using-CTAB-JGI.pdf>). Genomic DNA libraries were prepared, and samples were sequenced at 2  $\times$  151 bp length using the Illumina NextSeq platform at Microbial Genome Sequencing Center (MiGS, <https://www.migscenter.com/>). For the founder strains other than CC-1690, their sequenced reads were downloaded from NCBI. The quality of sequenced reads of

evolved strains and founders was examined by FastQC and trimmed using Trimmomatic-0.36 (*options*: HEADCROP:16 LEADING:30 TRAILING:28 SLIDINGWINDOW:4:15 MINLEN:54). Paired reads were mapped to the Joint Genome Institute v5.5 assembly of the *C. reinhardtii* CC503 mt+ genome (Merchant et al. 2007) using BWA-MEM default setting (Li 2013). Genomic variants (small polymorphisms such as SNPs [single nucleotide polymorphisms], indels [insertions and deletions], MNPs [multi-nucleotide polymorphisms], and complex events [composite insertion and substitution events]) were detected using FreeBayes v1.0.2-29 (*options*: -p 1 -m 3 -q 1) (Garrison and Marth 2012). Variants with quality scores greater than 20, read depth greater than 5x, and allele frequencies greater than 0.85 were analyzed. According to a previous study (Flowers et al. 2015), each founder strain contains a genome fingerprint that distinguish them from each other (e.g. see Flowers et al. 2015; Fig. 2b). Our approach was to generate a filtered genetic variant dataset that consisted of nonreference variants observed in all strains together, and identify ancestral identities of multicellular isolates using strain-specific variants along with mating types in founder strains.

## Supplementary Material

Supplementary material is available at *Genome Biology and Evolution* online.

## Acknowledgments

This work was supported by NASA Ames Research Center NNA17BB05A (Rosenzweig PI, Herron co-I), NASA Planetary Sciences Division 80NSSC20K0621 (Rosenzweig PI), and NASA Planetary Sciences Division 80NSSC23K1357 (Rosenzweig PI). The authors thank Ozan Bozdog and Alireza Zamani-Dahaj in the Ratcliff lab for useful discussion and for their assistance with epifluorescence microscopy, and Brandon Ross for his assistance with adding captions to time-lapse videos. We also thank Peter Conlin, Ross Lindsey, and Emily Cook for their helpful comments on earlier drafts of this manuscript. This material is based upon work while MDH was serving at the National Science Foundation.

## Funding

This work was supported by NASA Ames Research Center NNA17BB05A (NASA Astrobiology Institute) NASA Planetary Sciences Division 80NSSC20K0621 (Exobiology), and NASA Planetary Sciences Division 80NSSC23K1357 (Interdisciplinary Consortia for Astrobiology Research).

## Conflict of Interest

The authors have no conflicts of interest to declare.

## Data Availability

Sequencing data were deposited at the NCBI Sequence Read Archive with project number PRJNA820479 and accession number SAMN27009621-4.

## Literature Cited

- Albani A E, Mangano MG, Buatois LA, Bengtson S, Riboulleau A, Bekker A, Konhauer K, Lyons T, Rollion-Bard C, Bankole O, et al. Organism motility in an oxygenated shallow-marine environment 2.1 billion years ago. *Proc Natl Acad Sci U S A*. 2019;116(9):3431–3436. <https://doi.org/10.1073/pnas.1815721116>.
- Andersson SG, Zomorodipour A, Andersson JO, Sicheritz-Ponten T, Alsmark UC, Podowski RM, Näslund AK, Eriksson A-S, Winkler HH, Kurland CG. The genome sequence of *Rickettsia prowazekii* and the origin of mitochondria. *Nature*. 1998;396(6707):133–140. <https://doi.org/10.1038/24094>.
- Becks L, Ellner SP, Jones LE, Hairston NG Jr. Reduction of adaptive genetic diversity radically alters eco-evolutionary community dynamics. *Ecol Lett*. 2010;13(8):989–997. <https://doi.org/10.1111/j.1461-0248.2010.01490.x>.
- Bjorkman J, Samuelsson P, Andersson DI, Hughes D. Novel ribosomal mutations affecting translational accuracy, antibiotic resistance and virulence of *Salmonella typhimurium*. *Mol Microbiol*. 1999;31(1):53–58. <https://doi.org/10.1046/j.1365-2958.1999.01142.x>.
- Blount ZD, Barrick JE, Davidson CJ, Lenski RE. Genomic analysis of a key innovation in an experimental *Escherichia coli* population. *Nature*. 2012;489(7417):513–518. <https://doi.org/10.1038/nature11514>.
- Blount ZD, Borland CZ, Lenski RE. Historical contingency and the evolution of a key innovation in an experimental population of *Escherichia coli*. *Proc Natl Acad Sci U S A*. 2008;105(23):7899–7906. <https://doi.org/10.1073/pnas.0803151105>.
- Bonner JT. The origins of multicellularity. *Integr Biol*. 1998(1):27–36. [https://doi.org/10.1002/\(SICI\)1520-6602\(1998\)1:1<27::AID-INBI4>3.0.CO;2-6](https://doi.org/10.1002/(SICI)1520-6602(1998)1:1<27::AID-INBI4>3.0.CO;2-6).
- Bonner JT. First signals: the evolution of multicellular development. Princeton (NJ): Princeton University Press; 2000.
- Bonner JT. Why size matters: from bacteria to blue whales. Princeton (NJ): Princeton University Press; 2011.
- Boraas ME, Seale DB, Boxhorn JE. Phagotrophy by a flagellate selects for colonial prey: a possible origin of multicellularity. *Evol Ecol*. 1998;12(2):153–164. <https://doi.org/10.1023/A:1006527528063>.
- Boswell J, Lindsey CR, Cook E, Rosenzweig F, Herron M. Cryopreservation of clonal and polyclonal populations of *Chlamydomonas reinhardtii*. *Biol Methods Protoc*. 2021;6(1):bpab011. <https://doi.org/10.1093/biomethods/bpab011>.
- Brunet T, King N. The origin of animal multicellularity and cell differentiation. *Dev Cell*. 2017;43(2):124–140. <https://doi.org/10.1016/j.devcel.2017.09.016>.
- Cooper TF, Rozen DE, Lenski RE. Parallel changes in gene expression after 20,000 generations of evolution in *Escherichia coli*. *Proc Natl Acad Sci U S A*. 2003;100(3):1072–1077. <https://doi.org/10.1073/pnas.0334340100>.
- Du Q, Kawabe Y, Schilde C, Chen ZH, Schaap P. The evolution of aggregative multicellularity and cell-cell communication in the Dictyostelia. *J Mol Biol*. 2015;427(23):3722–3733. <https://doi.org/10.1016/j.jmb.2015.08.008>.
- Featherston J, Arakaki Y, Hanschen ER, Ferris PJ, Michod RE, Olson BJS, Nozaki H, Durand PM. The 4-celled *Tetrabaena socialis* nuclear genome reveals the essential components for genetic control of cell number at the origin of multicellularity in the volvocine lineage. *Mol Biol Evol*. 2018;35(4):855–870. <https://doi.org/10.1093/molbev/msx332>.

- Fisher KJ, Buskirk SW, Vignogna RC, Marad DA, Lang GI. Adaptive genome duplication affects patterns of molecular evolution in *Saccharomyces cerevisiae*. *PLoS Genet*. 2018;14(5):e1007396. <https://doi.org/10.1371/journal.pgen.1007396>.
- Flowers JM, Hazzouri KM, Pham GM, Rosas U, Bahmani T, Khraiwesh B, Nelson DR, Jijakli K, Abdrabu R, Harris EH, et al. Whole-genome resequencing reveals extensive natural variation in the model green alga *Chlamydomonas reinhardtii*. *Plant Cell*. 2015;27(9):2353–2369. <https://doi.org/10.1105/tpc.15.00492>.
- Gallaher SD, Fitz-Gibbon ST, Glaesener AG, Pellegrini M, Merchant SS. *Chlamydomonas* genome resource for laboratory strains reveals a mosaic of sequence variation, identifies true strain histories, and enables strain-specific studies. *Plant Cell*. 2015;27(9):2335–2352.
- Garrison E, Marth G. Haplotype-based variant detection from short-read sequencing. arXiv 1207.3907. <https://doi.org/10.48550/arXiv.1207.3907>, 20 July 2012, preprint: not peer reviewed.
- Gibson TM, Shih PM, Cumming VM, Fischer WW, Crockford PW, Hodgskiss MSW, Wörndle S, Creaser RA, Rainbird RH, Skulski TM, et al. Precise age of *Bangiomorpha pubescens* dates the origin of eukaryotic photosynthesis. *Geology*. 2018;46(2):135–138. <https://doi.org/10.1130/G39829.1>.
- Gorman DS, Levine RP. Cytochrome f and plastocyanin: their sequence in the photosynthetic electron transport chain of *Chlamydomonas reinhardtii*. *Proc Natl Acad Sci U S A*. 1965;54(6):1665–1669. <https://doi.org/10.1073/pnas.54.6.1665>.
- Gould SJ. Wonderful life: the Burgess Shale and the nature of history. New York City (NY): W. W. Norton & Co; 1989.
- Grosberg RK, Strathmann RR. The evolution of multicellularity: a minor major transition? *Annu Rev Ecol Syst*. 2007;38(1):621–654. <https://doi.org/10.1146/annurev.ecolsys.36.102403.114735>.
- Gross CH, Ranum LP, Lefebvre PA. Extensive restriction fragment length polymorphisms in a new isolate of *Chlamydomonas reinhardtii*. *Curr Genet*. 1988;13(6):503–508.
- Hanschen ER, Marriage TN, Ferris PJ, Hamaji T, Toyoda A, Fujiyama A, Neme R, Noguchi H, Minakuchi Y, Suzuki M, et al. The *Gonium pectorale* genome demonstrates co-option of cell cycle regulation during the evolution of multicellularity. *Nat Commun*. 2016;7(1):11370. <https://doi.org/10.1038/ncomms11370>.
- Harris EH. The *Chlamydomonas* sourcebook. 2nd ed. Cambridge (MA): Academic Press; 2009.
- Herron MD. What are the major transitions? *Biol Philos*. 2021;36(1):1–19. <https://doi.org/10.1007/s10539-020-09773-z>.
- Herron MD, Borin JM, Boswell JC, Walker J, Chen ICK, Knox CA, Boyd M, Rosenzweig F, Ratcliff WC. De novo origins of multicellularity in response to predation. *Sci Rep*. 2019;9(1):2328. <https://doi.org/10.1038/s41598-019-39558-8>.
- Herron MD, Hackett JD, Aylward FO, Michod RE. Triassic origin and early radiation of multicellular volvocine algae. *Proc Natl Acad Sci U S A*. 2009;106(9):3254–3258. <https://doi.org/10.1073/pnas.0811205106>.
- Kilham SS, Kreeger DA, Lynn SG, Goulden CE, Herrera L. COMBO: a defined freshwater culture medium for algae and zooplankton. *Hydrobiologia*. 1998;377(1/3):147–159. <https://doi.org/10.1023/A:1003231628456>.
- King N. The unicellular ancestry of animal development. *Dev Cell*. 2004;7(3):313–325. <https://doi.org/10.1016/j.devcel.2004.08.010>.
- King N, Westbrook MJ, Young SL, Kuo A, Abedin M, Chapman J, Fairclough S, Hellsten U, Isogai Y, Letunic I, et al. The genome of the choanoflagellate *Monosiga brevicollis* and the origin of metazoans. *Nature*. 2008;451(7180):783–788. <https://doi.org/10.1038/nature06617>.
- Knoll AH. The multiple origins of complex multicellularity. *Annu Rev Earth Planet Sci*. 2011;39(1):217–239. <https://doi.org/10.1146/annurev.earth.031208.100209>.
- Knoll AH, Hewitt D. Phylogenetic, functional, and geological perspectives on complex multicellularity. In: Calcott B, Sterelny K, editors. *The major transitions in evolution revisited*. Cambridge (MA): The MIT Press; 2011. p. 251–270.
- Kvitek DJ, Sherlock G. Whole genome, whole population sequencing reveals that loss of signaling networks is the major adaptive strategy in a constant environment. *PLoS Genet*. 2013;9(11):e1003972. <https://doi.org/10.1371/journal.pgen.1003972>.
- Lang GI, Botstein D, Desai MM. Genetic variation and the fate of beneficial mutations in asexual populations. *Genetics*. 2011;188(3):647–661. <https://doi.org/10.1534/genetics.111.128942>.
- Lenski RE, Travisano M. Dynamics of adaptation and diversification: a 10,000-generation experiment with bacterial populations. *Proc Natl Acad Sci U S A*. 1994;91(15):6808–6814. <https://doi.org/10.1073/pnas.91.15.6808>.
- Lewontin R. The units of selection. *Annu Rev Ecol Syst*. 1970;1(1):1–18. <https://doi.org/10.1146/annurev.es.01.110170.000245>.
- Li H. Aligning sequence reads, clone sequences and assembly contigs with BWA-MEM. arXiv 1303.3997. <https://doi.org/10.48550/arXiv.1303.3997>, 16 March 2013, preprint: not peer reviewed.
- Lindsey CR, Knoll AH, Herron M, Rosenzweig F. Fossil-calibrated molecular clock data enable reconstruction of steps leading to differentiated multicellularity and anisogamy in the volvocine algae. *BMC Biol*. 2024;22(1):79. <https://doi.org/10.1186/s12915-024-01878-1>.
- Lindsey CR, Rosenzweig F, Herron MD. Phylotranscriptomics points to multiple independent origins of multicellularity and cellular differentiation in the volvocine algae. *BMC Biol*. 2021;19(1):182. <https://doi.org/10.1186/s12915-021-01087-0>.
- Losos JB. Adaptive radiation, ecological opportunity, and evolutionary determinism. *American Society of Naturalists E. O. Wilson award address*. *Am Nat*. 2010;175(6):623–639. <https://doi.org/10.1086/652433>.
- Ma X, Shi X, Wang Q, Zhao M, Zhang Z, Zhong B. A reinvestigation of multiple independent evolution and Triassic-Jurassic origins of multicellular volvocine algae. *Genome Biol Evol*. 2023;15(8):evad142. <https://doi.org/10.1093/gbe/evad142>.
- Maisnier-Patin S, Berg OG, Liljas L, Andersson DI. Compensatory adaptation to the deleterious effect of antibiotic resistance in *Salmonella typhimurium*. *Mol Microbiol*. 2002;46(2):355–366. <https://doi.org/10.1046/j.1365-2958.2002.03173.x>.
- Maynard Smith J, Szathmáry E. *The major transitions in evolution*. Oxford (UK): Oxford University Press; 1995.
- McGhee G. *Convergent evolution: limited forms most beautiful*. Cambridge (MA): The MIT Press; 2011.
- Merchant SS, Prochnik SE, Vallon O, Harris EH, Karpowicz SJ, Witman GB, Terry A, Salamov A, Fritz-Laylin LK, Maréchal-Drouard L, et al. The *Chlamydomonas* genome reveals the evolution of key animal and plant functions. *Science*. 2007;318(5848):245–250. <https://doi.org/10.1126/science.1143609>.
- Michod RE, Roze D. Cooperation and conflict in the evolution of multicellularity. *Heredity (Edinb)*. 2001;86(1):1–7. <https://doi.org/10.1046/j.1365-2540.2001.00808.x>.
- Morris SC. *Life's solution: inevitable humans in a lonely universe*. Cambridge (UK): Cambridge University Press; 2003.
- Paps J, Holland PWH. Reconstruction of the ancestral metazoan genome reveals an increase in genomic novelty. *Nat Commun*. 2018;9(1):1730. <https://doi.org/10.1038/s41467-018-04136-5>.
- Prochnik SE, Umen J, Nedelcu AM, Hallmann A, Miller SM, Nishii I, Ferris P, Kuo A, Mitros T, Fritz-Laylin LK, et al. Genomic analysis of organismal complexity in the multicellular green alga *Volvox carteri*. *Science*. 2010;329(5988):223–226. <https://doi.org/10.1126/science.1188800>.
- Proschold T, Harris EH, Coleman AW. Portrait of a species: *Chlamydomonas reinhardtii*. *Genetics*. 2005;170(4):1601–1610.

- Quandt EM, Deatherage DE, Ellington AD, Georgiou G, Barrick JE. Recursive genomewide recombination and sequencing reveals a key refinement step in the evolution of a metabolic innovation in *Escherichia coli*. *Proc Natl Acad Sci U S A*. 2014;111(6):2217–2222. <https://doi.org/10.1073/pnas.1314561111>.
- Quandt EM, Gollihar J, Blount ZD, Ellington AD, Georgiou G, Barrick JE. Fine-tuning citrate synthase flux potentiates and refines metabolic innovation in the Lenski evolution experiment. *eLife*. 2015;4:e09696. <https://doi.org/10.7554/eLife.09696>.
- Ratcliff WC, Denison RF, Borrello M, Travisano M. Experimental evolution of multicellularity. *Proc Natl Acad Sci U S A*. 2012;109(5):1595–1600. <https://doi.org/10.1073/pnas.1115323109>.
- Ratcliff WC, Herron MD, Howell K, Pentz JT, Rosenzweig F, Travisano M. Experimental evolution of an alternating uni- and multicellular life cycle in *Chlamydomonas reinhardtii*. *Nat Commun*. 2013;4(1):2742. <https://doi.org/10.1038/ncomms3742>.
- Sack L, Zeyl C, Bell G, Sharbel T, Reboud X, Bernhardt T, Koelewyn H. Isolation of four new strains of *Chlamydomonas reinhardtii* (Chlorophyta) from soil samples. *J Phycol*. 1994;30:770–773.
- Sager R. Inheritance in the green alga *Chlamydomonas reinhardtii*. *Genetics*. 1955;40(4):476–489.
- Sager R, Granick S. Nutritional control of sexuality in *Chlamydomonas reinhardtii*. *J Gen Physiol*. 1954;37(6):729–742. <https://doi.org/10.1085/jgp.37.6.729>.
- Schrag SJ, Perrot V. Reducing antibiotic resistance. *Nature*. 1996;381(6578):120–121. <https://doi.org/10.1038/381120b0>.
- Schrag SJ, Perrot V, Levin BR. Adaptation to the fitness costs of antibiotic resistance in *Escherichia coli*. *Proc Biol Sci*. 1997;264(1386):1287–1291. <https://doi.org/10.1098/rspb.1997.0178>.
- Sebe-Pedros A, Ballare C, Parra-Acero H, Chiva C, Tena JJ, Sabidó E, Gómez-Skarmeta JL, Di Croce L, Ruiz-Trillo I. The dynamic regulatory genome of *Capsaspora* and the origin of animal multicellularity. *Cell*. 2016;165(5):1224–1237. <https://doi.org/10.1016/j.cell.2016.03.034>.
- Sebe-Pedros A, Degnan BM, Ruiz-Trillo I. The origin of Metazoa: a unicellular perspective. *Nat Rev Genet*. 2017;18(8):498–512. <https://doi.org/10.1038/nrg.2017.21>.
- Spanier J, Graham J, Jarvik J, Harris EH. Isolation and preliminary characterization of three *Chlamydomonas* strains interfertile with *Chlamydomonas reinhardtii* (Chlorophyta). *J Phycol*. 1992;28:822–828.
- Suga H, Chen Z, de Mendoza A, Sebe-Pedros A, Brown MW, Kramer E, Carr M, Kerner P, Vervoort M, Sánchez-Pons N, et al. The *Capsaspora* genome reveals a complex unicellular prehistory of animals. *Nat Commun*. 2013;4(1):2325. <https://doi.org/10.1038/ncomms3325>.
- Tang Q, Pang K, Yuan X, Xiao S. A one-billion-year-old multicellular chlorophyte. *Nat Ecol Evol*. 2020;4(4):543–549. <https://doi.org/10.1038/s41559-020-1122-9>.
- Tarnita CE, Taubes CH, Nowak MA. Evolutionary construction by staying together and coming together. *J Theor Biol*. 2013;320:10–22. <https://doi.org/10.1016/j.jtbi.2012.11.022>.
- Tikhonenkov DV, Hehenberger E, Esaulov AS, Belyakova OI, Mazei YA, Mylnikov AP, Keeling PJ. Insights into the origin of metazoan multicellularity from predatory unicellular relatives of animals. *BMC Biol*. 2020;18(1):39. <https://doi.org/10.1186/s12915-020-0762-1>.
- Umen J, Herron MD. Green algal models for multicellularity. *Annu Rev Genet*. 2021;55(1):603–632. <https://doi.org/10.1146/annurev-genet-032321-091533>.
- Wang Z, Wu M. An integrated phylogenomic approach toward pinpointing the origin of mitochondria. *Sci Rep*. 2015;5(1):7949. <https://doi.org/10.1038/srep07949>.
- Weinreich DM, Watson RA, Chao L. Perspective: sign epistasis and genetic constraint on evolutionary trajectories. *Evolution*. 2005;59(6):1165–1174. <https://doi.org/10.1111/j.0014-3820.2005.tb01768.x>.
- Zamora I, Feldman JL, Marshall WF. PCR-based assay for mating type and diploidy in *Chlamydomonas*. *Biotechniques*. 2004;37(4):534–536. <https://doi.org/10.2144/04374BM01>.

Associate editor: John Archibald